Open-circuit dissolution of platinum from the cathode in polymer electrolyte membrane water electrolysers

J. Dodwell[a], M. Maier[a], J. Majasan[a], R. Jervis[a], L. Castanheira[b], P. Shearing[a], G. Hinds[b], D.J.L. Brett[a]*

[a] *Electrochemical Innovation Lab, Department of Chemical Engineering, UCL, London, WC1E 7JE, United Kingdom*

[b] *National Physical Laboratory, Hampton Road, Teddington, Middlesex, TW11 0LW, UK*

* *Corresponding author. Tel.: +44 (0)20 7679 3310; fax: +44 (0)20 7383 2348. E-mail address: d.brett@ucl.ac.uk (D.J.L. Brett).*

1. Abstract

Platinum is the state-of-the-art catalyst for hydrogen evolution in polymer electrolyte membrane (PEM) water electrolysers; however, its stability has only been characterized to a limited extent *in situ*. This study measures platinum dissolving from the cathode during intermittent operation of a 3-electrode PEM electrolyser cell, using a differential pulse voltammetry technique that provided detection limits for platinum of less than 2 ng L^{-1}. Water samples were periodically taken during on-off current cycling, and during periods of open-circuit voltage (OCV) platinum dissolution was detected when the cathode potential rose above 0.85 V vs NHE due to diffusion of oxygen from the anode. This reached a maximum dissolution rate at the highest cathode potential of 1.02 V vs NHE, and gradually decayed over a 90 h period. The average total amount of platinum dissolved per 90 h OCV period was estimated to be 152 ng cm^{-2} or 0.005 % of the initial electrode catalyst mass. The dissolution mechanism was predicted to be the same as that occurring in PEM fuel cell cathodes, although being kinetically hindered in PEM electrolysers by the slow diffusion of oxygen from the anode to the cathode.

Keywords: PEM water electrolyser; Differential pulse voltammetry; ICP-MS; Platinum Dissolution; 3-electrode cell; Accelerated Stress Test

2. Introduction

One of the essential elements of the 'Hydrogen Economy' is the coupling of renewable energy resources to water electrolysers. In this way, hydrogen may be produced with very little associated carbon dioxide emissions, either from the hydrogen generation process itself or from the electrical energy source. When integrated into an electricity grid, electrolysers have a dual function as both a hydrogen generation system and as a grid balancing device, operating mainly during periods of excess grid electricity [1,2]. Electrolyser systems must therefore be highly resilient to fluctuations of power and rapid start-up and shut-down, whilst exhibiting only limited losses in performance [3,4].

The most commonly reported method of establishing durability is to monitor cell voltage under constant load; under which conditions, state-of-the-art polymer electrolyte membrane water electrolysers (PEMWEs) have been shown to exhibit excellent performance [5] with demonstrated lifetimes over 20,000 h [6]. The main lifetime limiting factors of PEMWEs under such conditions are usually found to be membrane thinning [7,8], poisoning of the membrane or cathode electrocatalyst due to metal dissolution and redeposition [9], or loss of performance due to the degradation of the anode electrocatalyst [10]. The effect of intermittent operation on the PEMWE and its components is, however, less commonly reported, and there seem to be two main reasons for this. Firstly, for novel PEMWE materials, *in situ* constant current measurements of performance are often the only necessary test, as immediate comparisons to other materials can be made [11,12]. Durability is much less often the subject of study with novel materials. In cases where it is, the performance losses are normally large enough that a prediction of lifetime can be extrapolated with accuracy within short timeframes [13–17]. Secondly, establishing a load cycling profile that is representative of real-world operation is complex, as factors such as operational currents and the frequency of changes in load, temperature and pressure may all have to be factored into the profile [18]. Some PEMWE materials have therefore not been as intensively studied as components for other systems, such as fuel cells, and important new findings are still being made.

An example of a relevant recent advance is the work of Weiß et al. [19] who determined that intermittent operation of a PEMWE causes an increase in contact resistance. This was explained to

be caused by passivation of the titanium gas diffusion layer, and the surface reduction of the iridium oxide Oxygen Evolution Reaction (OER) electrocatalyst to a less electronically conductive hydrous iridium oxide species [20]. This work demonstrated that the performance change caused by these mechanisms was induced by the open-circuit voltage (OCV) period. Brightman et al. [21] performed a similar intermittent operation study, with the focus being on the cathode. It was shown that intermittent operation caused a ~30 % loss of electrochemical surface area (ECSA) of the Pt Hydrogen Evolution Reaction (HER) electrocatalyst under a voltage cycling regime aimed at representing start-stop conditions. Using a PEMWE cell containing an *in situ* reference electrode the study also demonstrated that the cathode potential increased significantly during the OCV period, experiencing changes in potential similar to polymer electrolyte membrane (PEM) fuel cell electrodes [22]. This finding indicates that the HER electrocatalyst in PEMWEs may be susceptible to similar degradation mechanisms to the electrodes in PEM fuel cells: electrochemical Ostwald ripening, particle coalescence and agglomeration, dissolution of the Pt electrocatalyst, and detachment of the Pt from its carbon support [23–26].

The dissolution of Pt electrocatalysts is a well-documented phenomenon in fuel cells, where the process of dissolution and subsequent redeposition of Pt results in detectable bands of deposited Pt in the membrane [27,28]. Recent studies reporting on the use of inductively coupled plasma-mass spectrometry (ICP-MS) by flowing electrolyte in a scanning flow cell ICP-MS (SFC-ICP-MS) have demonstrated a powerful new method for measuring dissolution; providing near real-time measurements with extremely low limits of detection of dissolution from electrodes under electrochemical control [29–31]. SFC-ICP-MS studies with crystalline Pt and nanoparticle Pt/C working electrodes have shown that dissolution occurs at potentials close to the Pt-PtO_x redox potential [32]. This was shown to be a transient phenomenon, with dissolution rates measured at the redox potential, then decaying steadily with the further increase or decrease in electrode potential. In a series of studies by Topalov et al. [33,34] these findings were further developed and it was determined that dissolution occurring during the oxidative sweep was a result of either direct Pt dissolution or dissolution of the formed oxide layer. The accompanying, and greater, dissolution rate during the reductive sweep was proposed to be due to the formation of sub-surface oxides,

weakening the Pt – Pt bonds and thus promoting Pt dissolution. The increased depth of the oxide layer also was found to cause greater dissolution on reduction. The amount of dissolved Pt was also correlated with the electrode scan rate [33]. It was shown that, whilst only a minor correlation between the anodic scan rate and the anodic dissolution rate exists, there is a strong negative correlation between the cathodic scan rate and cathodic dissolution, with a six-fold increase in dissolution when the scan rate was reduced from 500 mV s^{-1} to 5 mV s^{-1}.

Real-time measurement of dissolution in electrochemical systems has proved to be a step-change in this field of research; however, because of complexity and high cost, in-line ICP-MS is not a readily available technique. In this study, we instead present Pt dissolution data measured by differential pulse voltammetry (DPV) using a hanging mercury drop electrode (HMDE) [35–37]. When an aqueous solution containing dissolved Pt is mixed with formaldehyde and hydrazine and an appropriate potential is applied to the HMDE (known as the pre-concentration step), an adsorbed Pt complex is formed on the mercury surface that catalyses the HER. The potential of the HMDE is then swept in the negative direction, where the maximum rate of HER is observed as a current peak (the catalytic wave) correlating to the amount of Pt adsorbed on the mercury surface and therefore the concentration of dissolved Pt in the sample [38]. The concentration is then determined by the method of standard additions. This DPV method is capable of detecting concentrations in the ng L^{-1} range [35], which is comparable to ICP-MS but at a fraction of the capital and operational costs, and also does not require training beyond that of typical practical electrochemistry. The DPV technique was used in this work to detect and quantify the effect of operational and OCV conditions on the dissolution of Pt from the HER electrocatalyst in the cathode of a conventional PEMWE. Although platinum black (PtB) is rarely used as the cathode catalyst in commercial PEMWE systems, it was chosen for this investigation over the more commercially relevant Pt/C, so that Pt losses arising from carbon support corrosion did not need to be considered. In this report, the electrolyser tests were performed with an ambient pressure PEMWE cell containing a Luggin capillary (a design modified from that reported on by Brightman et al. [21]), which allowed the separation of the PEMWE cell voltage into the anode and cathode potentials. As a first test, the cathode was held at a series of potentials increasing stepwise between -0.07 V and 1 V NHE, a range equal to the cathode potential

range at OCV shown in the report by Brightman. Outlet water samples were taken from the cathode at each potential step, and these samples were quantified both by DPV and ICP-MS for platinum dissolution. Secondly, on-off current cycles were performed on the PEMWE cell. Water samples here were taken from the cathode periodically during both operation and OCV. Pt dissolution in these samples was quantified by DPV only.

This work reports a number of important findings for the field of electrocatalysts in PEM electrolysers. To the best of our knowledge, this is the first time that DPV has been used to quantify electrocatalyst dissolution from an electrochemical device. This is also the first reported case of quantified Pt dissolution from an operating PEMWE cell. The findings show that whilst Pt dissolution from the Pt electrode is not expected to be a lifetime limiting factor with the loadings used in this report, at loadings more typical of state-of-the-art PEM electrolysers and future Pt-thrifted electrode formulations [5] dissolution may become a greater concern. The dissolution rates observed in this report may therefore be seen as the lower bound of estimated Pt loss from the electrode during OCV. These results may also act as a guide for the development of PEM electrolyser accelerated stress tests (ASTs), which are designed to cause degradation representative of long-term operation within a short timeframe [39]. These results show that Pt dissolution needs to be considered when developing an AST, and that to be representative of cathode degradation under normal operation the AST must be based on OCV rather than voltage control.

3. Experimental

3.1. Catalyst ink and Catalyst Coated Membrane (CCM) production

Both PtB and iridium oxide inks were made following the same recipe. 1 g of PtB (Sigma Aldrich 520780, 25-34 m^2 g^{-1}) or iridium oxide (Alfa Aesar 43396) was mixed with 1 mL deionised water (18.2 MΩ cm) and 0.01 g polyacrylic acid solution (Sigma-Aldrich 52395, 35 wt % in water). The slurry was then stirred until the catalyst was fully wetted. To this, 5 g of Nafion dispersion was added (D521, 5 wt % Nafion dispersion in 45 % water) and mixed so that a ratio by mass of 4:1 catalyst: Nafion solids was achieved. This mass ratio was chosen as it volumetrically has approximately similar

ratios to the more standard Pt/C: Nafion ratios, which are more commonly around 2:1 [40]. After further mixing, 4 mL more deionised water was added, followed by 5 mL isopropyl alcohol (IPA, Sigma Aldrich W292907). The ink was then dispersed in an ultrasonic bath for a minimum of 30 minutes.

Catalyst inks were hand-sprayed using a Spraycraft SP30KC spray gun onto pre-weighed 5 mil (127 µm) glass-reinforced Teflon sheets on a hotplate set at 90 °C. A 5 cm^2 circular mask was placed over the Teflon sheet in order to produce a defined spray geometry. During spraying the substrate was periodically weighed on a 4-point analytical balance to give an accurate measure of the mass gain and hence the catalyst loading. Once the appropriate catalyst loading had been achieved, a 16 cm^2 Nafion 117 membrane (Fuel Cell Store 591239) was sandwiched between the sprayed catalyst layers, with a further Teflon substrate and a pressure distributing felt backing each catalyst-sprayed Teflon sheet. This sandwich was placed into a hot press (Bungard) at 140 °C. A pressure of 6 bar was applied for 5 minutes, after which the composite was removed from the press and left to cool. The Teflon layers were peeled off the Nafion, leaving the catalyst layers laminated on the Nafion membrane to produce the CCM. The CCMs were then soaked in 125 mL 0.5 M H_2SO_4 for a minimum of 24 h before use. Final CCM loadings were determined to be 3 mg cm^{-2} IrO_x and 3 mg cm^{-2} PtB.

3.2. PEMWE cell testing

Details of the 3-electrode PEMWE cell design can be found in the supporting information (S.I.1). Electrochemical impedance spectroscopy (EIS) measurements were taken at a series of current densities in order to determine iR drop (S.I.2). No significant iR drop was evident, so the electrochemical measurements in this report have not been iR corrected. Electrochemical tests were controlled by a Gamry Interface 5000 potentiostat. Both anode and cathode were fed continuously with deionised water (18.2 MΩ cm), preheated so that the inlet water temperature was 60 °C, at a

rate of 5 mL cm^{-2} min^{-1} throughout each test. Water samples at the cathode inlet and outlet were taken periodically for DPV and ICP-MS analysis. Unless otherwise stated, all potentials in this work are reported against the normal hydrogen electrode (NHE).

Tests at constant cathode potential were performed to produce water samples for the comparative ICP-MS and DPV analysis, and to provide a comparison with the OCV tests. The 3-electrode design of the PEMWE cell allowed the cathode potential to be directly controlled while flushing the anode with nitrogen-purged water. The cathode was held at a series of potentials against the reference electrode increasing stepwise from -0.07 V to 1 V, with each potential being held for 2 minutes in order to produce enough water sample to be tested by both ICP-MS and DPV.

The OCV tests consisted of a period of operation at 1 A cm^{-2} for 1 h (1 A cm^{-2} pre - OCV), followed by OCV for 72 h, followed by operation at 1 A cm^{-2} for a further 1 h (1 A cm^{-2} post-OCV). The cathode potential was monitored with time during the OCV tests. Cyclic voltammetry (CV) measurements were performed before and after the OCV test under the same conditions in order to investigate any changes in electrochemical performance of the cathode. CV was performed at 20 mV s^{-1} between the cathode and reference electrode between 0.03 V and 1 V NHE. The OCV test was performed three times in sequence on the same CCM, with the complete data set available in S.I.4.

3.3. DPV technique

DPV of Pt was performed on a VA 797 Computrace (Metrohm UK). The electrochemical cell consisted of an HMDE working electrode, Ag/AgCl reference electrode and glassy carbon counter electrode. The supporting electrolyte consisted of 0.7 M sulfuric acid (Sigma Aldrich 339741), 6.7 mM formaldehyde (Sigma Aldrich 252549) and 3 mM hydrazine sulfate (Sigma Aldrich 455865). 1.5 mL of supporting electrolyte was pipetted into the electrochemical cell with 9 mL deionized water (18.2 MΩ cm) and 1 mL of sample. The hydrazine reduces any Pt(IV) species to Pt(II), and the reaction of hydrazine and formaldehyde forms formaldehyde hydrazone, which can complex Pt(II) to form a positively charged Pt(II) - hydrazone complex. The voltammetric technique for the determination of

Pt concentration comprises pre-concentration of the Pt complex by adsorption on the surface of the HMDE, followed by DPV in the HER region. The experimental parameters for the test are given in Table 1. For quantification of dissolved Pt concentration the method of standard additions was used; two DPV sweeps were taken at the initial concentration, followed by two sweeps with one standard addition of 10 µL of 1 µg L^{-1} Pt solution, followed by a further two sweeps with a final addition of the same concentration and volume. From this the initial concentration was calculated from a line of best fit. Representative DPV sweeps and the line of best fit can be found in S.I.3.

Table 1. Experimental parameters for the determination of dissolved Pt concentration by DPV.

Parameter	
Pre-concentration step	
Stirring rate, *r*	600 rpm
Pre-concentration potential	-0.6 V (Ag/AgCl | 3 M KCl)
Pre-concentration duration	120 s
Equilibration duration	10 s
DPV sweep	
Start potential	-0.6 V (Ag/AgCl | 3 M KCl)
End potential	-1.1 V (Ag/AgCl | 3 M KCl)
Potential step	0.006 V
Step time	0.3 s
Sweep rate	0.02 V s^{-1}
Pulse amplitude	0.05 V
Characteristic catalytic wave potential	-0.88 V (Ag/AgCl | 3 M KCl)

Due to the recirculation of the cathode water all samples taken at the inlet contained a background concentration of Pt of order ≈7 ng L^{-1}. To determine the concentration arising from Pt dissolution from the catalyst layer, the values measured at the cathode outlet were corrected by subtracting the concentration measured at the cathode inlet immediately prior to the cathode outlet measurement. This corrected value was then converted into a Pt dissolution rate (ng cm^{-2} h^{-1}) with respect to the geometric surface area of the CCM.

3.4. ICP-MS

The DPV results were compared against results obtained from ICP-MS measurements (Varian 820-MS, USA). The samples were conditioned with 1 % HNO_3 to stabilise elements in the solution, and

were calibrated against $PtCl_6^{2-}$ standards of 0.2 – 20 ng L^{-1}. Further details on the calibration can be found in S.I.3.

4. Results and discussion

4.1. Comparison of ICP-MS and DPV

Cathode potential hold tests were performed at potentials ranging from -0.07 V (the potential of the cathode during operation at 1 A cm^{-2}) to 1 V (the maximum potential that the cathode reaches during OCV). This range was determined by the OCV plot in the report by Brightman et al. [21], and was here explained to be due to the diffusion of oxygen through the membrane from the anode. The OCV plot in this report (Figure 2) gave a similar cathode potential transition. Samples of outlet water were taken and their Pt concentration was measured by both ICP-MS and DPV, as shown in Figure 1. It is clear from the size of the error bars that the typical concentration of Pt arising from cathode dissolution was too low for meaningful quantification by the available ICP-MS. In contrast, DPV was able to quantify Pt dissolution at this level, making this technique well-suited for quantification of dissolved Pt in PEMWEs. A limit of detection test, shown in Figure S.I.4, similarly demonstrates that DPV was sensitive to Pt(IV) species at concentrations as low as 2 ng L^{-1}, but ICP-MS was only sensitive from 50 ng L^{-1} upwards. Unlike ICP-MS, the DPV technique is not sensitive to Pt(0) however, and cannot therefore detect Pt lost by erosion, or corrosion of the electrode support (if one were to be used, i.e. Pt/C). Although there are high associated standard deviations with ICP-MS results in Figure 1, and so any difference between ICP-MS and DPV values cannot be determined with any statistical significance here, the generally higher recorded dissolution values may be an indication of the contribution of Pt(0) to the ICP-MS recorded dissolution value. It should be noted here that this comparison concerns only the two specific instruments used in this work, and should not be taken as a general comparison between ICP-MS and DPV for Pt sensitivity. The ICP-MS device used here has higher limits of detection in comparison to state-of-the-art ICP-MS instruments, which may be in the

range of 0.001 - 0.1 ng L^{-1} [41]. Likewise, the sensitivity of the DPV measurements may be improved upon, and the limits quoted here do not represent absolute detection limits. A similar comparison study on biological samples was performed by Zimmerman et al., who reported limits of detection for Pt of 1 ng L^{-1} using ICP-MS and 0.13 ng L^{-1} for DPV [42].

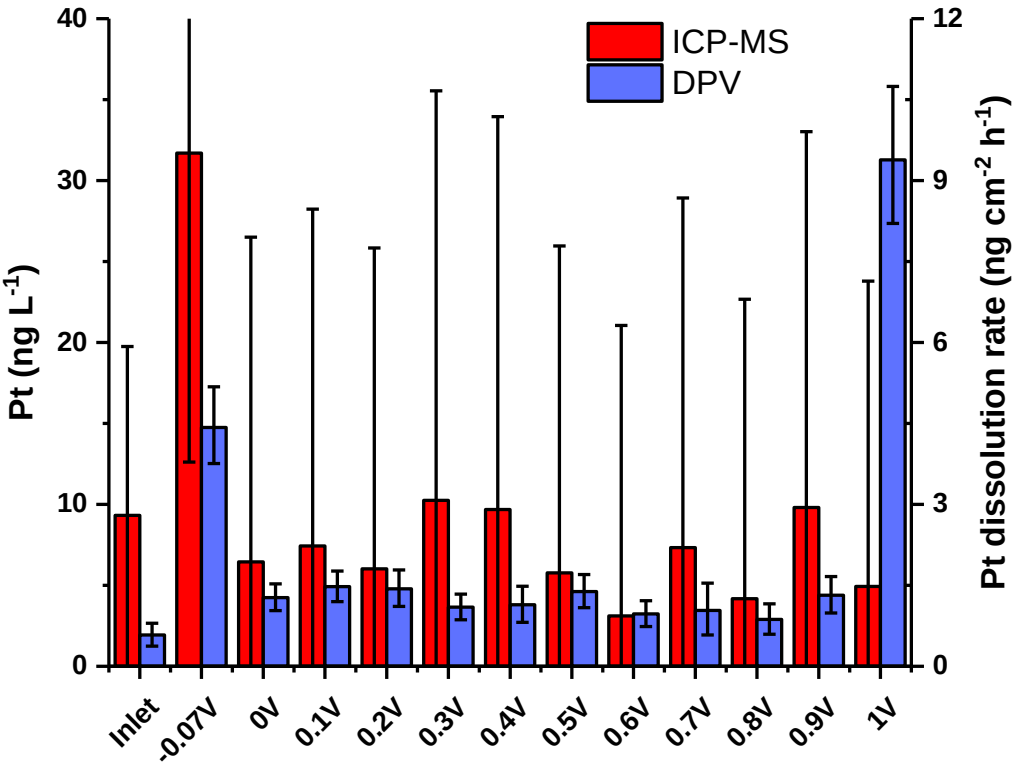

Figure 1. Dissolved Pt concentration in PEMWE cathode water as a function of cathode potential, measured by ICP-MS and DPV. Note that for the cathode outlet measurements from -0.07 V to 1 V, the background Pt concentration at the cathode inlet has been subtracted. The error bars represent the first standard deviation. With the ICP-MS results, the standard deviation is based on the average of 5 separate measurements. With the DPV results, the standard deviation is the standard deviation of the line of best fit, which was measured from 6 points. Note the samples were taken immediately after potential change, and so for -0.07V the high dissolution value can be explained to be a transient effect. This effect is also shown in Figure 3c.

Figure 1 also shows that the Pt concentration of the outlet water at a cathode potential of -0.07 V is significantly higher than samples taken at the other potentials. The cause of this is the same as that shown in Figure 3c; a high but rapidly diminishing concentration of Pt is measured from the onset of operation. The -0.07 V sample was taken after only 1 minute of operation, and so is high for the

same reasons. The underlying cause of this high initial Pt concentration is discussed in the following section.

4.2. OCV test

The evolution of cathode potential with time during the OCV test is shown in Figure 2 (red line), with the anode potential and cell voltage also included for reference. In this setup, with water flowing at the cathode, the cathode potential during operation at 1 A cm^{-2} was -0.07 V. Upon commencement of the OCV period, the potential increased from -0.002 V to 1.02 V in about 5 h and remained steady at this high potential for the remainder of the 72 h period. This was found to be repeatable for the three OCV tests performed, as shown in Figure S.I.8.

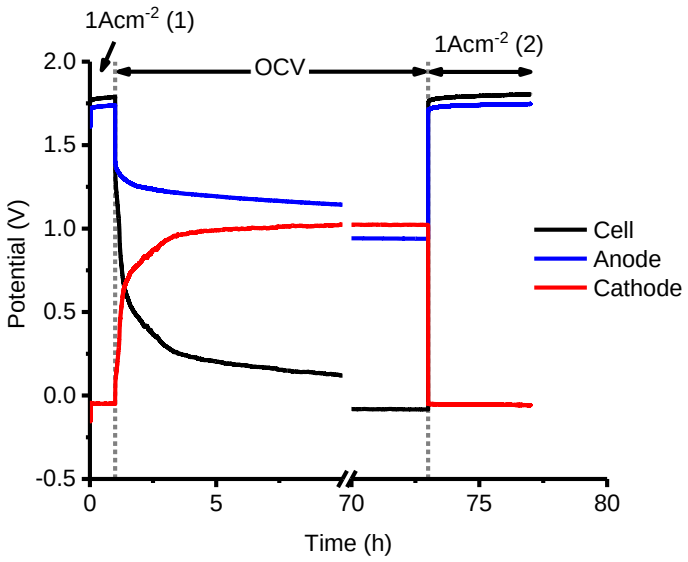

Figure 2. Evolution of cathode potential, anode potential and cell voltage with time during the OCV test. The electrolyser was operated at 1 A cm^{-2} for 1 h, followed by a 72 h OCV period, followed by operation at 1 A cm^{-2} again for 1 h.

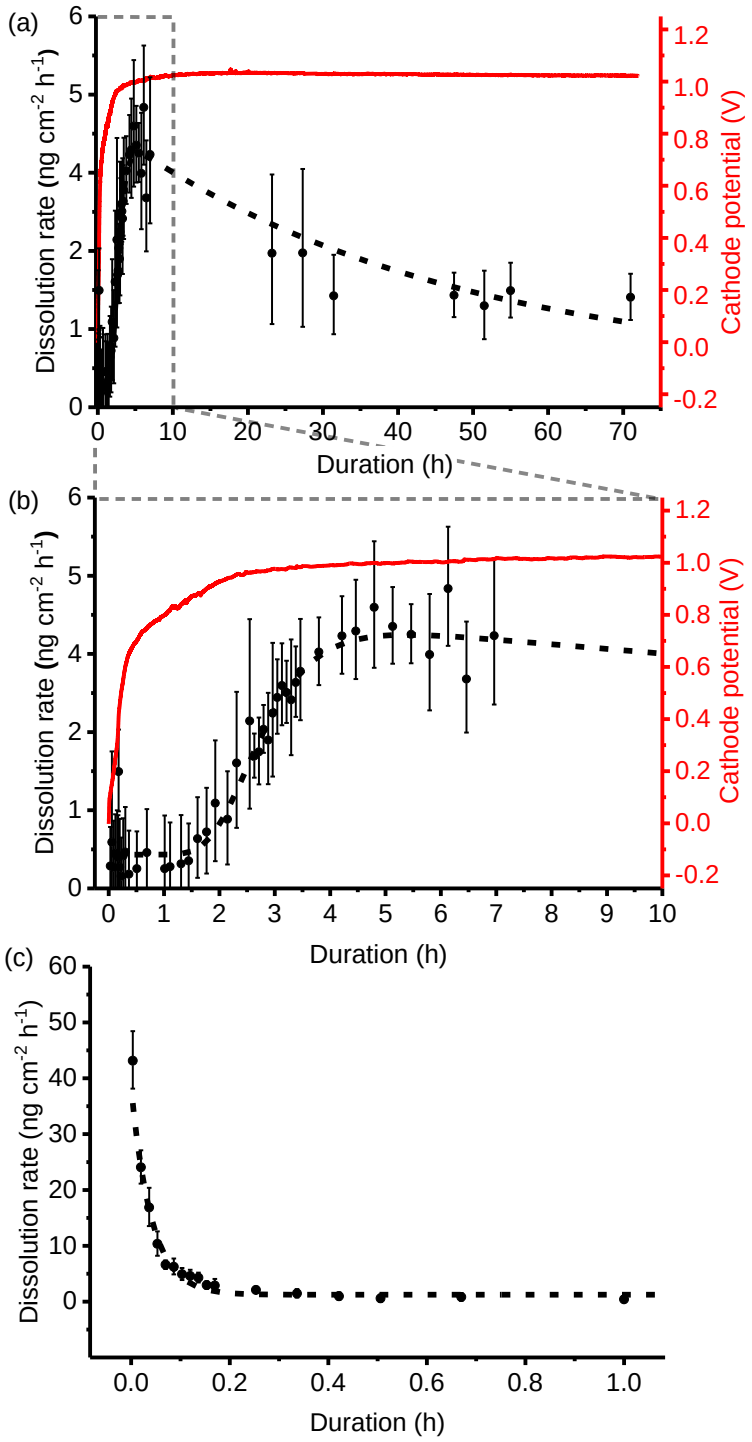

Figure 3. Platinum dissolution rate from the PEMWE cathode during OCV test 1. Shown in (a) is the dissolution rate from the full duration of the OCV test with (b) showing the rate during the first 10 h. The cathode potential is shown in red. (c) is the Pt dissolution rate from the onset of operation at 1 A cm^{-2} immediately after the OCV period. The dotted line is the best fit to the data, and details of this fitting can be found in S.I.5. The dissolution dataset on all three OCV plots can be found in S.I.4.

The rate of Pt dissolution from the cathode during the OCV portion of OCV test 1 is shown in Figure 3a and b. From the onset of the OCV period every measurement showed net Pt dissolution (i.e. the outlet concentration of Pt was always higher than the inlet concentration). During the first 1.5 h of OCV, the dissolution rate was measurable, but the standard deviations of the individual measurements were too large for it to be stated with confidence that the dissolution rate was positive. However, it can be assumed that the dissolution rate is constant during this period (i.e. no other dissolution mechanism is occurring), and so the dissolution values in this period may be averaged. In the case of OCV test 1 the dissolution rate was 0.51 ng $cm^{-2}\,h^{-1}$, with a lower confidence interval of 0.34 ng $cm^{-2}\,h^{-1}$ and upper confidence interval of 0.68 ng $cm^{-2}\,h^{-1}$. Following on from this constant rate, dissolution increased to a maximum after approximately 5 h and then decayed slowly over the remainder of the 72 h OCV period. This maximum in dissolution rate coincides with the attainment of a steady-state cathode potential due to diffusion of oxygen from the anode. Plotting the dissolution rate as a function of cathode potential, in Figure 4, indicates that the onset of dissolution occured between 0.85 V - 0.90 V, which is in good agreement with SFC-ICP-MS literature [33].

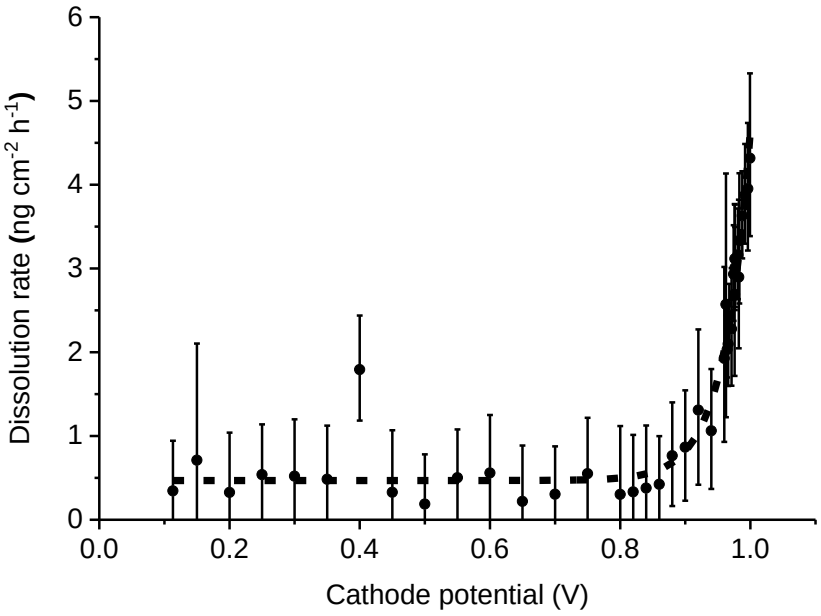

Figure 4. Pt dissolution as a function of increasing cathode potential in a PEMWE. Data taken from OCV test 1. Similar trends are observed for all three OCV tests (Figure S.I.10).

The Pt dissolution rate was also measured during operation at 1 A cm^{-2} immediately following the OCV period (Figure 3c). At the onset of operation, the rate of Pt dissolution was an order of magnitude higher than the maximum rate at OCV, but then decayed rapidly within approximately 30 minutes. There are two potential explanations for this additional dissolution phenomenon. Firstly, as the cathode has built up a surface Pt-oxide layer during the OCV period, the switch to the cathodic potential of operation could invoke dissolution due to reduction of the oxidised Pt surface and the competition between this and surface dissolution [33]. However, this effect is only significant at low sweep rates and in PEMWEs, with the extremely rapid potential step in cathode potential from OCV to operation, a large dissolution rate caused by this mechanism would not be expected. A second, and more likely explanation is that this instantaneous increase in apparent dissolution rate is an artefact caused by the displacement of the higher Pt concentration solution in the GDL by the evolution of hydrogen gas produced at the start of operation. This could also explain the higher apparent dissolution rate during the brief operation period at a constant potential of -0.07 V (Figure 1).

4.3. Effect of Pt dissolution on electrode lifetime

The Pt dissolution data, as shown in Figure 3 and Figure S.I.9, make it possible to estimate the lifetime of the PtB electrode under the given test conditions. The dotted lines in these Figures show a best-fit estimate of the OCV Pt dissolution fitted to a pulse profile, and an exponential decay function fitted to the dissolution at the onset of operation (see S.I.5 for fitting details). The following calculations were made using the averaged pulse profile of the OCV dissolution profiles (see Figure S.I.9d). This fitting was made with two considerations. Firstly, it was assumed that the background dissolution rate was constant throughout the OCV and operation period, and was unaffected by cathode potential or the increase in the concentration of dissolved Pt close to the electrode surface. Secondly, as the Pt averaged dissolution rate at OCV was still statistically significant after 72 h, the best-fit profile and confidence ranges were extended to the point at which the lower confidence interval reached the averaged background dissolution rate of 0.49 ng cm^{-2} h^{-1}. This is the point at which it can no longer be stated with confidence that potential-induced Pt dissolution is still occurring. In the case of the averaged profile in Figure S.I.9d, this was determined to be 90 h.

Integration of the averaged OCV dissolution profile gives the total amount of Pt dissolved per cm^2 for each OCV test. This gave a mean value of 152 ng cm^{-2}, with lower and upper confidence intervals of 80 ng cm^{-2} and 214 ng cm^{-2} respectively. For this particular CCM/PtB combination, the percentage of Pt lost from the electrode during an OCV period lasting 90 h is around 0.005 %. This corresponds to about 20,000 on-off cycles until complete Pt dissolution, although the performance loss of the electrode would be likely to precede this as a certain amount of Pt is of course needed for adequate HER kinetics. It should be noted that this value does not take into account Pt lost by mechanical means and cannot be correlated to catalyst layer performance losses by Ostwald ripening or particle agglomeration [43].

The dissolution rates observed in Figure 3, and the ensuing calculations, should not be used as an absolute reference for the predicted Pt electrode lifetime, but they do serve a useful purpose in

highlighting the substantial effect that different intermittent operational regimes may have on the Pt electrode.

The amount of Pt dissolved during on-off cycling will naturally depend on the duration of the OCV period, with less Pt dissolved per cycle with a shorter OCV period. However, with the OCV period being shorter, the time taken for a complete on-off cycle is reduced accordingly. In principle, the duration of operation is also a factor that can influence lifetime due to the operational background dissolution rate, measured at 2.31 ng cm^{-2} h^{-1} for these particular conditions. However, the total amount of dissolved Pt measured under the peak during operation (Figure 3c) is relatively small at only 1.5 ng cm^{-2}, and so does not contribute significantly to the overall dissolution. As the Pt dissolution rate at OCV is not constant, the duration of the OCV period has an impact upon how rapidly over time Pt dissolves, which has implications for the overall lifetime of the cathode. An estimation of the time averaged dissolution rate from the PtB electrode under a range of on-off operational regimes is given in Figure 5. From extrapolation of the average dissolution and operation dissolution data, the most damaging intermittent operation mode is a cycle of operation for 0.01 h (the shortest duration calculated), followed by an OCV period of 7.9 h. This provides an average dissolution rate of 3.60 ng cm^{-2} h^{-1} with lower and upper confidence intervals of 1.76 and 5.88 ng cm^{-2} h^{-1} respectively. Conversely, the mode of operation which will reduce the degradation the most, and hence extend lifetime by the greatest extent, is an operation period of 0.01 h followed by an OCV period of 0.2 h. In this case the average dissolution rate is 0.59 ng cm^{-2} h^{-1} with lower and upper confidence intervals of 0.45 and 1.33 ng cm^{-2} h^{-1} respectively. Such short operational periods are not reflective of realistic operational conditions, however the dissolution rate is found to be relatively insensitive to the operational duration and is much more dependent on the OCV duration. With an operation period of 1 hour, the maximum dissolution rate is on average 3.48 ng cm^{-2} h^{-1} with lower and upper limits of 1.73 and 5.62 ng cm^{-2} h^{-1} respectively. Only at much longer operation times (>10 h) does the operation time substantially alter the average dissolution rate.

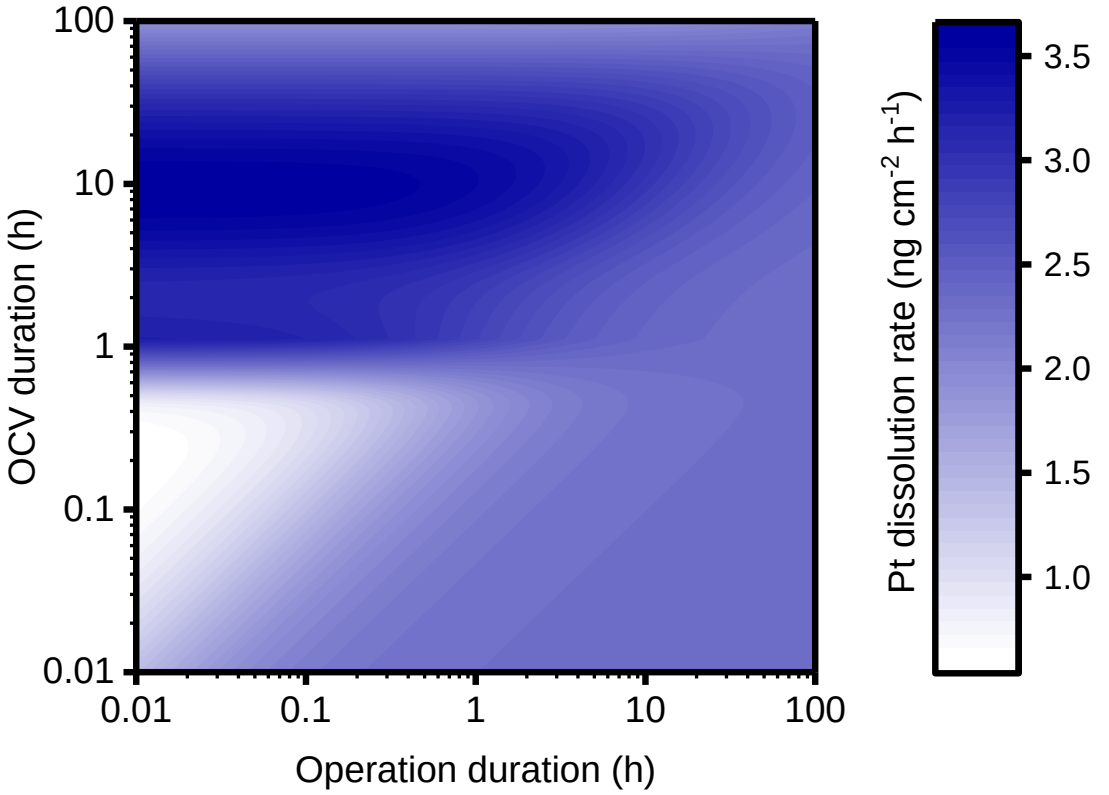

Figure 5. Average Pt dissolution rate as a function of the duration of operation versus the duration of the OCV period. The dissolution rate during operation is constant, but dissolution at OCV is dependent on the potential and duration of OCV. In the case of the PtB OCV test the most damaging on-off regime was found to be a short operation (<0.01h) followed by a 17.9 h OCV period. The average dissolution rate at this point is 3.60 ng cm^{-2} h^{-1}. Performing the same analysis against the lower and upper confidence intervals of the plot (Figure S.I.9d) gives 1.76 ng cm^{-2} h^{-1} and 5.88 ng cm^{-2} h^{-1} respectively.

If it were assumed that Pt dissolution is the only degradation mechanism occuring on the CCM, and that performance loss would only occur once the Pt has completely dissolved from the cathode, then the lifetime of the CCM tested in this report (3 mg cm^{-2} PtB) is estimated to be 95 years, with a lower and upper confidence limit of 58.3 and 194 years, respectively. With reduction of the Pt to a more commercially relevant loading (0.5 mg cm^{-2} Pt for example [5]) dissolution may become a more significant degradation mechanism, with the estimated time for complete dissolution at 16 years instead. This estimation however does not take into account the minimum required Pt loadings for adequate performance, and does not account for the other degradation mechanisms which may also reduce ECSA. 95 years of lifetime may therefore stand as an upper limit of lifetime for the 3 mg cm^{-2}

Pt cathode in this report and 16 years for a cathode at 0.5 mg cm^{-2}. These results are of importance when developing accelerated stress tests (ASTs) which mimic long-term degradation of the PEMWE within short timeframes. As can be seen here, a short duration of OCV seems to cause the least Pt loss by dissolution and therefore gives the longest lifetime estimate. Under the conditions studied in this work, the most damaging AST would be one that operates the cell for a very short time period and then holds the cell at OCV for 7.9 h. In comparison to an OCV period of 10 min, the degradation by Pt dissolution during a 7.9 h OCV period is accelerated by a factor of 5.

A further complication when considering AST development is the method by which the cathode potential is controlled during the off period of the cycle. There are two possible ways to manipulate the cathode potential during this period: through OCV, where the cathode potential is free to adjust depending on the balance of hydrogen and oxygen concentrations at the electrode surface; or potential control, where the cathode potential is held constant by an external source, such as a potentiostat. At OCV, the cathode potential rises to more oxidising potentials due to diffusion of oxygen from the anode (Figure 2), while under potential control it is often fixed [21].

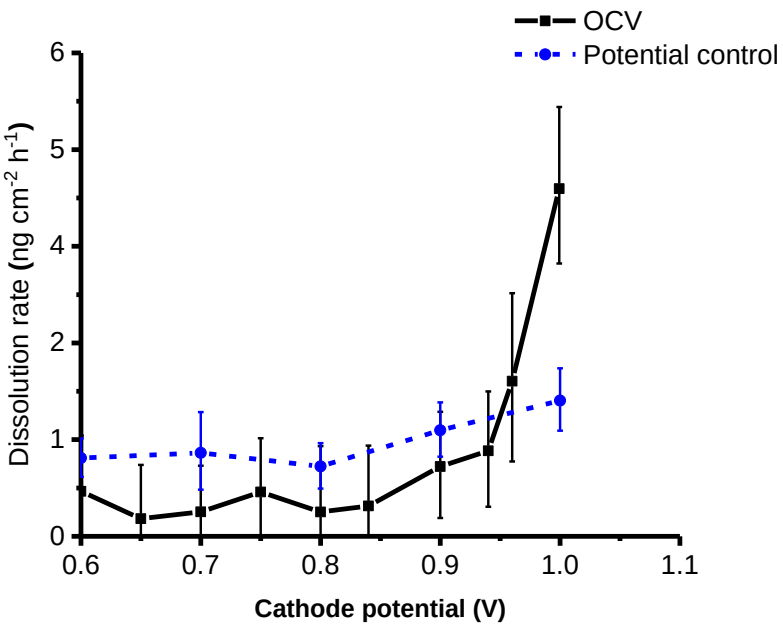

Figure 6. Comparison of Pt dissolution rates for the cathode at OCV and under potential control. The data in this graph is a combination of the potential control data in Figure 1 and OCV data in Figure 4.

Comparison of Pt dissolution rate at OCV versus dissolution under potential control is given in Figure 6. Under potential control, the dissolution rate does not show the same marked increase above 0.9 V that is evident in the OCV plot. This therefore shows that, despite being at similar potentials, the early stages of OCV where the cathode potential rises induces a greater rate of dissolution than the equivalent potential under potential control. This does not mean that no transient dissolution process occurs under potential control, as the resolution of the sampling (1 sample at each potential after holding for 1 minute) will have precluded observation of such a peak. However, the lack of onset of increased dissolution with increasing potential under potential control is in agreement with SFC-ICP-MS reports [33,44]. The cause of the greater dissolution during OCV is expanded on in Section 4.5.

4.4. PtB surface changes

CV measurements of the PtB electrode reveal interesting structural changes occurring as a result of the OCV test. Shown in Figure 7 are CV measurements taken before the OCV test 1 (BoT) and after (EoT). Measurement of the electrochemical surface area (ECSA) from the integration of the hydrogen underpotential deposition (H_{upd}) peaks shows that the OCV period had an impact upon the ECSA, which decreased from 319 cm^2_{Pt} cm^{-2} to 261 cm^2_{Pt} cm^{-2}, approximating an 18 % loss of the active surface area. It can furthermore be seen that the magnitudes of the H_{upd} peaks corresponding to hydrogen adsorption at the Pt(100) step sites were proportionally more reduced in comparison to Pt(110), indicating that the Pt dissolution rate may be higher with the more active, and therefore more labile, active sites [45]. This 18 % loss of ECSA does not correspond with the total platinum lost from the cathode during the OCV test however. From the dissolution analysis approximately only 0.005 % of the catalyst was dissolved, and so the large loss of ECSA clearly represents the loss of surface atoms only.

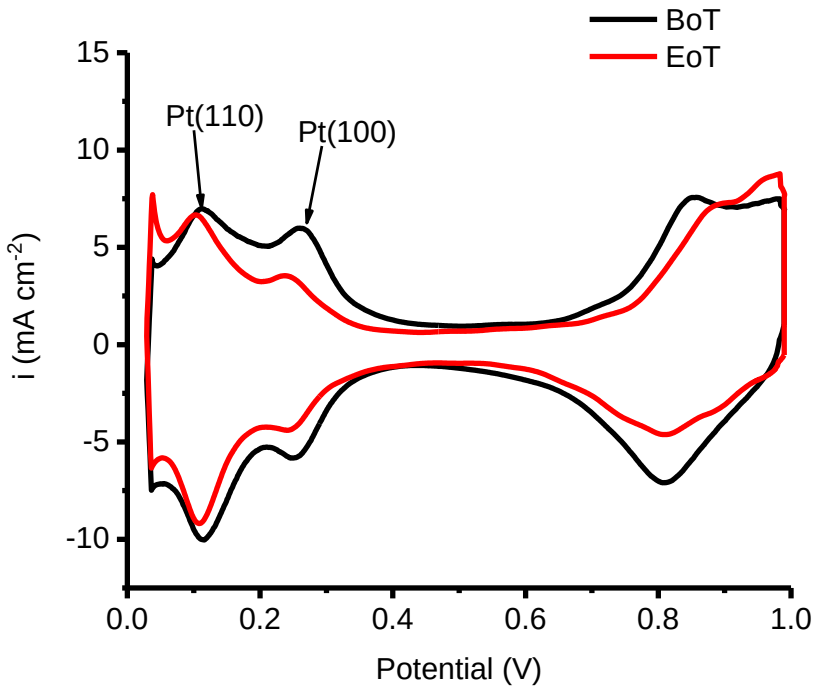

Figure 7. Cyclic voltammetry of PtB cathode before OCV test (BoT) and after the 72 h OCV period (EoT) of OCV test 1. Highlighted are the peaks associated with the Pt(100) and Pt(110) H_{upd} step sites.

4.5. Mechanisms of Pt dissolution in PEMWE cathodes

The mechanisms of Pt dissolution in PEMWE cathodes are likely to be similar in nature to those in PEM fuel cells [46]. These include electrochemical dissolution of Pt (1), and the formation of an oxide film (2) followed by chemical reduction to Pt^{2+} (3) [47].

$$Pt \rightarrow Pt^{2+} + 2e^{-} \qquad E_0\,(Pt/Pt^{2+}) = 1.188\ V + 0.0295 \log\,(Pt^{2+}) \qquad (1)$$

$$Pt + H_2O \rightarrow PtO + 2H^{+} + 2e^{-} \qquad E_0(Pt/PtO) = 0.98\ V - 0.59pH \qquad (2)$$

$$PtO + 2H^{+} \rightarrow Pt^{2+} + H_2O \qquad \log(Pt^{2+}) = -7.06 - 2pH \qquad (3)$$

Reaction (1) was reported by Cherevko et al. [32] as occurring at potentials as low as 0.85 V on Pt, correlating well with the onset of dissolution observed in this study. It has been noted that, since the equilibrium potential of this reaction is dependent on the surface concentration of Pt^{2+} species, the

equilibrium potential becomes more positive as dissolution proceeds, and thus the reaction should be self-limiting at the surface of a fuel cell electrocatalyst [44]. However, in a PEMWE the presence of water flowing through the cathode may prevent the surface concentration of Pt^{2+} on the electrode from increasing to the point where the equilibrium potential is significantly changed. This reaction may therefore be more significant in PEMWEs than in PEM fuel cells, and could contribute to the dissolution observed. Even with this dissolution reaction, the place exchange of Pt and OH species would occur, eventually forming an oxide layer and thus decreasing the dissolution rate over time. This would provide a rationale for the observed decrease in dissolution rate over the OCV period, and is consistent with the explanation of transient dissolution of Pt given by Topalov et al. [33]. The production of protons through reactions (2) and (3) may, however, contribute to the observed Pt dissolution. Yadav et al. [48] reported on this matter on high surface area Pt electrodes, and determined that reaction (2) is suppressed at lower pH due to the elevated equilibrium potential, therefore favouring reaction (1). The lower pH may also promote reaction (3), again resulting in an overall increase in Pt dissolution. However, the pH shift due to the reaction may be relatively small for the same reasons given to explain the increased Pt dissolution in PEMWEs compared to PEMFC; due to the presence of water at the cathode, the volume into which the protons are migrating is large and therefore the change in concentration may not shift the equilibrium potential substantially. Furthermore, as evidence suggests that Nafion has a pH of between -0.08 and 1.4 [49–51] the effect of a slight increase in proton concentration may not significantly alter the equilibria of reactions (2) and (3). As it has been shown here that one of the factors which may impact the rate of Pt dissolution is the volume of water at the cathode, the dissolution rate may differ in PEMWEs where the cathode is operated ‘dry’ (without an active water flow through the cathode). The volume of water present at the cathode in ‘dry’ systems is variable, and is a function of the amount of water collecting in the cell due to electroosmosis, the length of time the cell is operated, and is even dependent on the cell design and orientation.

The rate at which dissolution occurs is likely to be due to the relative availability of oxygen at the cathode. Unlike PEM fuel cell cathodes, PEMWE cathodes are not oxygen-rich, and as such, Pt dissolution is likely to be correlated to the kinetics of oxygen diffusion through the membrane. [27,52–56].

5. Conclusions

For the first time, Pt dissolution from the cathode during intermittent operation of a PEMWE has been observed. Dissolution was analysed using DPV, a technique which shows promise as a cost-effective and highly sensitive method to detect dissolved Pt species in PEMWE cathode water, giving comparable limits of detection to ICP-MS. Pt dissolution has been shown to occur over a long timeframe with approximately 152 ng cm^{-2} of a 3 mg cm^{-2} PtB catalyst predicted to be lost during a 90 h OCV period, equivalent to 0.005 % of the total catalyst loading. This places the estimate of the lifetime of the studied catalyst layer at approximately 95.2 years, far in excess of the majority of other components in the PEMWE. This lifetime estimate is, however, only relevant for the PtB catalyst tested, and is likely to be substantially reduced for state-of-the-art Pt/C catalysts with loadings in the range 0.2 mg cm^{-2} - 0.5 mg cm^{-2} [5] due to the lower initial loadings involved. Method development for the DPV technique may allow for the separate speciation of Pt(0) from Pt(II) and Pt(IV), which would also provide information pertaining to the rate of Pt loss due to carbon support corrosion. The mechanism of this dissolution process is likely to be similar to that of the cathode catalyst in PEM fuel cells, in which the dissolution of Pt gradually becomes hindered by surface passivation. However, in PEMWEs it is anticipated that the Pt dissolution rate would be amplified due to the increased volume and flow rate of liquid water at the cathode. In addition, the kinetics of these reactions will be complicated by oxygen crossover from the anode, which is dependent on several factors including the thickness of the Nafion membrane, the distribution of vapour phase and dissolved gases, and their respective partial pressures. Finally, this work may highlight the need for consideration about how PEWME systems are managed when non-operational. Unlike AWE, where it is common practice to apply a ‘protecting current’ that protects the cell components against the

damaging potential swings of OCV [2], there is no information regarding performing the same in PEMWE. As one of the simple solutions to mitigate Pt dissolution would be to maintain a low cathode potential, then the application of a protecting current should be considered in this case. This does however have to be balanced against other considerations, such as the need to continuously draw power, and the possible promotion of other degradation mechanisms, such as peroxide formation [56].

Declaration of competing interests

The authors declare that they have no known competing financial interests or personal relationships that could have appeared to influence the work reported in this paper.

Acknowledgements

This work was supported by the National Measurement System of the UK Department for Business, Energy & Industrial Strategy. The authors would also like to acknowledge funding from the EPSRC (EP/L015277/1, EP/P009050/1, EP/M014371/1, EP/M009394/1, EP/M023508/1, EP/L015749/1, EP/N022971/1) for supporting hydrogen research in the Electrochemical Innovation Lab (EIL).

References

[1] M. Ball, M. Weeda, The hydrogen economy - Vision or reality?, Int. J. Hydrogen Energy. 40 (2015) 7903–7919. https://doi.org/10.1016/j.ijhydene.2015.04.032.

[2] A. Buttler, H. Spliethoff, Current status of water electrolysis for energy storage, grid balancing and sector coupling via power-to-gas and power-to-liquids: A review, Renew. Sustain. Energy Rev. 82 (2018) 2440–2454. https://doi.org/10.1016/j.rser.2017.09.003.

[3] A. Bergen, L. Pitt, A. Rowe, P. Wild, N. Djilali, Transient electrolyser response in a renewable-regenerative energy system, Int. J. Hydrogen Energy. 34 (2009) 64–70.

https://doi.org/10.1016/j.ijhydene.2008.10.007.

[4] L. Allidières, A. Brisse, P. Millet, S. Valentin, M. Zeller, On the ability of pem water electrolysers to provide power grid services, Int. J. Hydrogen Energy. 44 (2019) 9690–9700. https://doi.org/10.1016/j.ijhydene.2018.11.186.

[5] M. Carmo, D.L. Fritz, J. Mergel, D. Stolten, A comprehensive review on PEM water electrolysis, Int. J. Hydrogen Energy. 38 (2013) 4901–4934. https://doi.org/10.1016/j.ijhydene.2013.01.151.

[6] K.E. Ayers, E.B. Anderson, C.B. Capuano, B.D. Carter, L.T. Dalton, G. Hanlon, J. Manco, M. Niedzwiecki, Research Advances Towards Low Cost, High Efficiency PEM Electrolysis, ECS Trans. 33 (2010) 3–15.

[7] S.A. Grigoriev, K.A. Dzhus, D.G. Bessarabov, P. Millet, Failure of PEM water electrolysis cells: Case study involving anode dissolution and membrane thinning, Int. J. Hydrogen Energy. 39 (2014) 20440–20446. https://doi.org/10.1016/j.ijhydene.2014.05.043.

[8] S. Siracusano, N. Van Dijk, R. Backhouse, L. Merlo, V. Baglio, A.S. Aricò, Degradation issues of PEM electrolysis MEAs, Renew. Energy. 123 (2018) 52–57. https://doi.org/10.1016/j.renene.2018.02.024.

[9] S. Stucki, G.G. Scherer, S. Schlagowski, E. Fischer, PEM water electrolysers: Evidence for membrane failure in 100 kW demonstration plants, J. Appl. Electrochem. 28 (1998) 1041–1049. https://doi.org/10.1023/A:1003477305336.

[10] C. Rozain, E. Mayousse, N. Guillet, P. Millet, Influence of iridium oxide loadings on the performance of PEM water electrolysis cells: Part I-Pure IrO2-based anodes, Appl. Catal. B Environ. 182 (2016) 153–160. https://doi.org/10.1016/j.apcatb.2015.09.013.

[11] H. Kim, E. Hwang, H. Park, B.-S. Lee, J.H. Jang, H.J. Kim, S.H. Ahn, S.-K. Kim, Non-precious metal electrocatalysts for hydrogen production in proton exchange membrane water

electrolyzer, Appl. Catal. B Environ. 206 (2017) 608–616. https://doi.org/10.1016/j.apcatb.2017.01.074.

[12] S. Siracusano, N. Van Dijk, E. Payne-Johnson, V. Baglio, A.S. Aricò, Nanosized IrOx and IrRuOx electrocatalysts for the O2evolution reaction in PEM water electrolysers, Appl. Catal. B Environ. 164 (2015) 488–495. https://doi.org/10.1016/j.apcatb.2014.09.005.

[13] S. Siracusano, V. Baglio, N. Van Dijk, L. Merlo, A.S. Aricò, Enhanced performance and durability of low catalyst loading PEM water electrolyser based on a short-side chain perfluorosulfonic ionomer, Appl. Energy. 192 (2017) 477–489. https://doi.org/10.1016/j.apenergy.2016.09.011.

[14] C. Rakousky, U. Reimer, K. Wippermann, M. Carmo, W. Lueke, D. Stolten, An analysis of degradation phenomena in polymer electrolyte membrane water electrolysis, J. Power Sources. 326 (2016) 120–128. https://doi.org/10.1016/j.jpowsour.2016.06.082.

[15] J.L. Corona-Guinto, L. Cardeño-García, D.C. Martínez-Casillas, J.M. Sandoval-Pineda, P. Tamayo-Meza, R. Silva-Casarin, R.G. González-Huerta, Performance of a PEM electrolyzer using RuIrCoOx electrocatalysts for the oxygen evolution electrode, Int. J. Hydrogen Energy. 38 (2013) 12667–12673. https://doi.org/10.1016/j.ijhydene.2012.12.071.

[16] L. Wang, V.A. Saveleva, S. Zafeiratos, E.R. Savinova, P. Lettenmeier, P. Gazdzicki, A.S. Gago, K.A. Friedrich, Highly active anode electrocatalysts derived from electrochemical leaching of Ru from metallic Ir0.7Ru0.3for proton exchange membrane electrolyzers, Nano Energy. 34 (2017) 385–391. https://doi.org/10.1016/j.nanoen.2017.02.045.

[17] S. Siracusano, V. Baglio, S.A. Grigoriev, L. Merlo, V.N. Fateev, A.S. Aricò, The influence of iridium chemical oxidation state on the performance and durability of oxygen evolution catalysts in PEM electrolysis, J. Power Sources. 366 (2017) 105–114. https://doi.org/10.1016/j.jpowsour.2017.09.020.

[18] F. Fouda-Onana, M. Chandesris, V. Médeau, S. Chelghoum, D. Thoby, N. Guillet, Investigation on the degradation of MEAs for PEM water electrolysers part I: Effects of testing conditions on MEA performances and membrane properties, Int. J. Hydrogen Energy. 41 (2016) 16627–16636. https://doi.org/10.1016/j.ijhydene.2016.07.125.

[19] A. Weiß, A. Siebel, M. Bernt, T.-H. Shen, V. Tileli, H.A. Gasteiger, Impact of Intermittent Operation on Lifetime and Performance of a PEM Water Electrolyzer, J. Electrochem. Soc. 166 (2019) F487–F497. https://doi.org/10.1149/2.0421908jes.

[20] E. Rasten, G. Hagen, R. Tunold, Electrocatalysis in water electrolysis with solid polymer electrolyte, Electrochim. Acta. 48 (2003) 3945–3952. https://doi.org/10.1016/j.electacta.2003.04.001.

[21] E. Brightman, J. Dodwell, N. Van Dijk, G. Hinds, In situ characterisation of PEM water electrolysers using a novel reference electrode, Electrochem. Commun. 52 (2015) 1–4. https://doi.org/10.1016/j.elecom.2015.01.005.

[22] J.A. Nogueira, K. Krischer, H. Varela, Coupled Dynamics of Anode and Cathode in Proton-Exchange Membrane Fuel Cells, ChemPhysChem. 20 (2019) 3081–3088. https://doi.org/10.1002/cphc.201900531.

[23] Z. Zhao, L. Castanheira, L. Dubau, G. Berthomé, A. Crisci, F. Maillard, Carbon corrosion and platinum nanoparticles ripening under open circuit potential conditions, J. Power Sources. 230 (2013) 236–243. https://doi.org/10.1016/j.jpowsour.2012.12.053.

[24] A. Pavlišič, P. Jovanovič, V.S. Šelih, M. Šala, N. Hodnik, M. Gaberšček, Platinum Dissolution and Redeposition from Pt/C Fuel Cell Electrocatalyst at Potential Cycling, J. Electrochem. Soc. 165 (2018) F3161–F3165. https://doi.org/10.1149/2.0191806jes.

[25] L. Castanheira, W.O. Silva, F.H.B. Lima, A. Crisci, L. Dubau, F. Maillard, Carbon Corrosion in Proton-Exchange Membrane Fuel Cells: Effect of the Carbon Structure, the Degradation

Protocol, and the Gas Atmosphere, (2015). https://doi.org/10.1021/cs501973j.

[26] R. Sharma, S. Gyergyek, Q. Li, S.M. Andersen, Evolution of the degradation mechanisms with the number of stress cycles during an accelerated stress test of carbon supported platinum nanoparticles, J. Electroanal. Chem. 838 (2019) 82–88. https://doi.org/10.1016/j.jelechem.2019.02.052.

[27] J. Zhang, B.A. Litteer, W. Gu, H. Liu, H.A. Gasteiger, Effect of Hydrogen and Oxygen Partial Pressure on Pt Precipitation within the Membrane of PEMFCs, J. Electrochem. Soc. 154 (2007) B1006. https://doi.org/10.1149/1.2764240.

[28] P.J. Ferreira, G.J. la O', Y. Shao-Horn, D. Morgan, R. Makharia, S. Kocha, H.A. Gasteiger, Instability of Pt⁄C Electrocatalysts in Proton Exchange Membrane Fuel Cells, J. Electrochem. Soc. 152 (2005) A2256. https://doi.org/10.1149/1.2050347.

[29] S. Cherevko, A.R. Zeradjanin, A.A. Topalov, N. Kulyk, I. Katsounaros, K.J.J. Mayrhofer, Dissolution of noble metals during oxygen evolution in acidic media, ChemCatChem. 6 (2014) 2219–2223. https://doi.org/10.1002/cctc.201402194.

[30] S. Cherevko, T. Reier, A.R. Zeradjanin, Z. Pawolek, P. Strasser, K.J.J. Mayrhofer, Stability of nanostructured iridium oxide electrocatalysts during oxygen evolution reaction in acidic environment, Electrochem. Commun. 48 (2014) 81–85. https://doi.org/10.1016/j.elecom.2014.08.027.

[31] P. Jovanovič, N. Hodnik, F. Ruiz-Zepeda, I. Arčon, B. Jozinović, M. Zorko, M. Bele, M. Šala, V.S. Šelih, S. Hočevar, M. Gaberšček, Electrochemical Dissolution of Iridium and Iridium Oxide Particles in Acidic Media: Transmission Electron Microscopy, Electrochemical Flow Cell Coupled to Inductively Coupled Plasma Mass Spectrometry, and X-ray Absorption Spectroscopy Study, J. Am. Chem. Soc. 139 (2017) 12837–12846. https://doi.org/10.1021/jacs.7b08071.

[32] S. Cherevko, G.P. Keeley, S. Geiger, A.R. Zeradjanin, N. Hodnik, N. Kulyk, K.J.J. Mayrhofer, Dissolution of Platinum in the Operational Range of Fuel Cells, ChemElectroChem. 2 (2015) 1471–1478. https://doi.org/10.1002/celc.201500098.

[33] A.A. Topalov, S. Cherevko, A.R. Zeradjanin, J.C. Meier, I. Katsounaros, K.J.J. Mayrhofer, Towards a comprehensive understanding of platinum dissolution in acidic media, Chem. Sci. 5 (2014) 631–638. https://doi.org/10.1039/C3SC52411F.

[34] A.A. Topalov, I. Katsounaros, M. Auinger, S. Cherevko, J.C. Meier, S.O. Klemm, K.J.J.J. Mayrhofer, Dissolution of Platinum: Limits for the Deployment of Electrochemical Energy Conversion ? Angewandte, Angew. Chemie - Int. Ed. 51 (2012) 12613–12615. https://doi.org/10.1002/anie.201207256.

[35] Z. Zhao, H. Freiser, Differential Pulse Polarographic Determination of Trace Levels of Platinum, Anal. Chem. 58 (1986) 1498–1501. https://doi.org/10.1021/ac00298a050.

[36] K. Hoppstock, F. Alt, K. Cammann, G. Weber, Determination of platinum in biotic and environmental materials part II: A sensitive voltammetric method, Fresenius Z Anal. Chemie. 335 (1989) 813–816. https://doi.org/10.1007/BF01204094.

[37] C.M.G. Van Den Berg, G.S. Jacinto, The determination of platinum in sea water by adsorptive cathodic stripping voltammetry, Anal. Chim. Acta. 211 (1988) 129–139. https://doi.org/10.1016/S0003-2670(00)83675-2.

[38] S.G. Mairanovskii, The theory of catalytic hydrogen waves in organic polarography, J. Electroanal. Chem. 6 (1963) 77–118. https://doi.org/10.1016/s0022-0728(63)80149-7.

[39] P. Aßmann, A.S. Gago, P. Gazdzicki, K.A. Friedrich, M. Wark, Toward developing accelerated stress tests for proton exchange membrane electrolyzers, Curr. Opin. Electrochem. 21 (2020) 225–233. https://doi.org/10.1016/j.coelec.2020.02.024.

[40] W. Xu, K. Scott, The effects of ionomer content on PEM water electrolyser membrane

electrode assembly performance, Int. J. Hydrogen Energy. 35 (2010) 12029–12037. https://doi.org/10.1016/j.ijhydene.2010.08.055.

[41] R. Komendova, Recent advances in the preconcentration and determination of platinum group metals in environmental and biological samples, Trends Anal. Chem. 122 (2020) 115708. https://doi.org/10.1016/j.trac.2019.115708.

[42] S. Zimmermann, C.M. Menzel, Z. Berner, J.D. Eckhardt, D. Stüben, F. Alt, J. Messerschmidt, H. Taraschewski, B. Sures, Trace analysis of platinum in biological samples: A comparison between sector field ICP-MS and adsorptive cathodic stripping voltammetry following different digestion procedures, Anal. Chim. Acta. 439 (2001) 203–209. https://doi.org/10.1016/S0003-2670(01)01041-8.

[43] Q. Feng, X.-Z. Yuan, G. Liu, B. Wei, Z. Zhang, H. Li, H. Wang, A review of proton exchange membrane water electrolysis on degradation mechanisms and mitigation strategies, J. Power Sources. 366 (2017) 33–55. https://doi.org/10.1016/j.jpowsour.2017.09.006.

[44] S. Cherevko, N. Kulyk, K.J.J. Mayrhofer, Durability of platinum-based fuel cell electrocatalysts: Dissolution of bulk and nanoscale platinum, Nano Energy. 29 (2016) 275–298. https://doi.org/10.1016/j.nanoen.2016.03.005.

[45] O. Diaz-Morales, T.J.P. Hersbach, C. Badan, A.C. Garcia, M.T.M. Koper, Hydrogen adsorption on nano-structured platinum electrodes, Faraday Discuss. 210 (2018) 301–315. https://doi.org/10.1039/c8fd00062j.

[46] R.M. Darling, J.P. Meyers, Kinetic Model of Platinum Dissolution in PEMFCs, J. Electrochem. Soc. 150 (2003) A1523–A1527. https://doi.org/10.1149/1.1613669.

[47] K. Sasaki, M. Shao, R. Adzic, Dissolution and stabilization of platinum in oxygen cathodes, 2009. https://doi.org/10.1007/978-0-387-85536-3_2.

[48] A.P. Yadav, T. Okayasu, Y. Sugawara, A. Nishikata, T. Tsuru, Effects of pH on Dissolution and

Surface Area Loss of Platinum Due to Potential Cycling, J. Electrochem. Soc. 159 (2012) C190–C194. https://doi.org/10.1149/2.065204jes.

[49] B. Seger, K. Vinodgopal, P. V. Kamat, Proton activity in Nafion films: Probing exchangeable protons with methylene blue, Langmuir. 23 (2007) 5471–5476. https://doi.org/10.1021/la0636816.

[50] M. Umeda, K. Sayama, T. Maruta, M. Inoue, Proton activity of Nafion 117 membrane measured from potential difference of hydrogen electrodes, Ionics (Kiel). 19 (2013) 623–627. https://doi.org/10.1007/s11581-012-0791-z.

[51] E. Brightman, D. Pasquier, Measurement and adjustment of proton activity in solid polymer electrolytes, Electrochem. Commun. 82 (2017) 145–149. https://doi.org/10.1016/j.elecom.2017.08.005.

[52] A. Kongkanand, J.M. Ziegelbauer, Surface platinum electrooxidation in the presence of oxygen, J. Phys. Chem. C. 116 (2012) 3684–3693. https://doi.org/10.1021/jp211490a.

[53] S. Mitsushima, Y. Koizumi, S. Uzuka, K.I. Ota, Dissolution of platinum in acidic media, Electrochim. Acta. 54 (2008) 455–460. https://doi.org/10.1016/j.electacta.2008.07.052.

[54] M. Schalenbach, T. Hoefner, P. Paciok, M. Carmo, W. Lueke, D. Stolten, Gas Permeation through Nafion. Part 1: Measurements, J. Phys. Chem. C. 119 (2015) 25145–25155. https://doi.org/10.1021/acs.jpcc.5b04155.

[55] M. Schalenbach, M.A. Hoeh, J.T. Gostick, W. Lueke, D. Stolten, Gas Permeation through Nafion. Part 2: Resistor Network Model, J. Phys. Chem. C. 119 (2015) 25156–25169. https://doi.org/10.1021/acs.jpcc.5b04157.

[56] F.N. Khatib, T. Wilberforce, O. Ijaodola, E. Ogungbemi, Z. El-Hassan, A. Durrant, J. Thompson, A.G. Olabi, Material degradation of components in polymer electrolyte membrane (PEM) electrolytic cell and mitigation mechanisms: A review, Renew. Sustain. Energy Rev. 111 (2019)

1–14. https://doi.org/10.1016/j.rser.2019.05.007.